

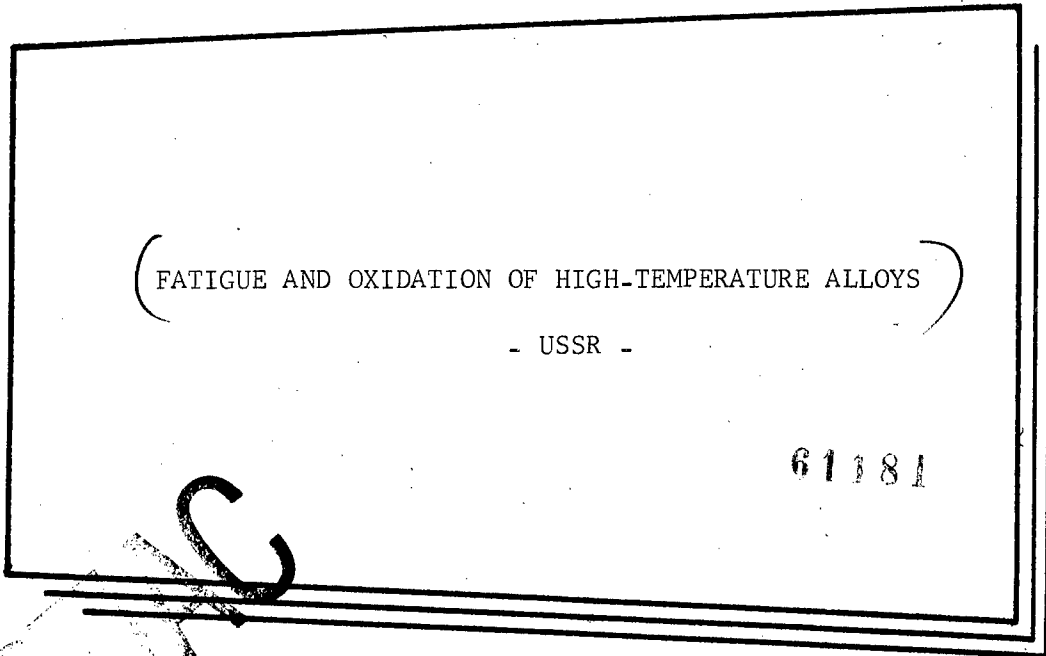
DMIC

JPRS: 24,826

TT: 64-31362

28 May 1964

ok.



( FATIGUE AND OXIDATION OF HIGH-TEMPERATURE ALLOYS )

- USSR -

61181

ALTERNATIVE

(SECOND PRINTING - 15 MARCH 1965)

20010906 053

U. S. DEPARTMENT OF COMMERCE

CLEARINGHOUSE FOR FEDERAL

SCIENTIFIC AND TECHNICAL INFORMATION

JOINT PUBLICATIONS RESEARCH SERVICE

Building Tempo E

East Adams Drive, 4th and 6th Streets, S. W.

Washington, D. C. 20443

**DISTRIBUTION STATEMENT A**

Approved for Public Release

Distribution Unlimited

Price: \$1.25

REPRODUCED FROM  
BEST AVAILABLE COPY

## F O R E W O R D

This publication was prepared under contract for the Joint Publications Research Service as a translation or foreign-language research service to the various federal government departments.

The contents of this material in no way represent the policies, views or attitudes of the U. S. Government or of the parties to any distribution arrangement.

### PROCUREMENT OF JPRS REPORTS

All JPRS reports may be ordered from the Clearinghouse for Federal Scientific and Technical Information. Reports published prior to 1 February 1963 can be provided, for the most part, only in photocopy (xerox). Those published after 1 February 1963 will be provided in printed form.

Details on special subscription arrangements for any JPRS report will be provided upon request.

All current JPRS reports are listed in the Monthly Catalog of U. S. Government Publications, available on subscription at \$4.50 per year (\$6.00 foreign), including an annual index, from the Superintendent of Documents, U. S. Government Printing Office, Washington 25, D. C.

All current JPRS scientific and technical reports are cataloged and subject-indexed in Technical Translations, published semimonthly by the Clearinghouse for Federal Scientific and Technical Information, and also available on subscription (\$12.00 per year domestic, \$16.00 foreign) from the Superintendent of Documents. Semiannual indexes to Technical Translations are available at additional cost.

## FATIGUE AND OXIDATION OF HIGH-TEMPERATURE ALLOYS

- USSR -

Following is a translation of four articles from the Russian-language book Voprosy fiziki metallov i metallovedeniya, Sbornik nauchnykh trudov Instituta metallofiziki, No. 17 (Problems of Metals Physics and Metals Science, Works of the Institute of Metals Physics, No. 17), Kiev, Publishing House of the Ukrainian Academy of Sciences, 1963. Complete bibliographic information accompanies each article.

## TABLE OF CONTENTS

	<u>Page</u>
Structure Changes During Unsteady Heating of Nozzle Vanes Made From a Cast, Nickel-Base Heat-Resisting Alloy . . . . .	1
Investigation of Crystal Structure Change During Thermal Fatigue of Alloy ZhS-6K . . . . .	13
Effect of Unsteady Heating on Change of Magnetic and Electrical Properties of Alloy ZhS-6K. . . . .	22
Study of the Diffusion and Oxidation Processes in Alloy ZhS-6K Under Conditions of Thermal Cycling . . . . .	35

STRUCTURE CHANGES DURING UNSTEADY HEATING OF  
NOZZLE VANES MADE FROM A CAST, NICKEL-BASE  
HEAT-RESISTING ALLOY

[Following is a translation of an article by V. N. Gridnev, A. I. Yefimov, N. P. Kushnareva, and M. S. Khazanov/in the Russian-language book Voprosy Fiziki Metallov i Metallovedeniya (Problems of Metals Physics and Metals Science), Collection of Scientific Works of the Institute of Metal Physics, No 17, Kiev, 1963, Academy of Sciences Ukrainian SSR, pp 98-110.]

[Nozzle<sup>A</sup> vanes of gas turbines operate under conditions of an unsteady temperature field. Thermal stresses forming during engine starts and stops lead to premature fracture of vanes due to the onset and development of thermal fatigue cracks [17]. In a number of works the decisive role of surface layers of heat-resisting alloys in opposing fracture at high temperatures and under conditions of unsteady heating is presented. It has also been established that cracks which form in the surface layers of intake vanes and sometimes in the discharge vanes are developed in grain boundaries. However, due to difficulties of an experimental nature (insignificant thickness of surface layers), until recently there was no systematic data on the effect of thermal cycling on phase composition and structure of surface layers of vanes under operating conditions. The present investigation is devoted to a study of the structure changes in surface layers and internal regions of samples and vanes of cast nimonic.]

to p. 13

Material and method of investigation

The items of investigation were nozzle vanes which had passed thermal fatigue tests on a dynamic-gas installation under conditions simulating starting and stopping of a gas turbine engine. Temperature mode of gas was 20-1200-20°C. Vanes

were investigated after a varying number of cycles in which the greatest number of cycles was 650.

Thermal cycling of samples (disks with a 16-mm diameter and 8-mm height) was done in a furnace as follows: heat to 1000 C in 30 seconds, hold at 1000 C for 4 min, cool in air stream or water. Structure changes occurring in the vanes and samples after thermal cycling were studied with ordinary and electron microscopes. In the investigation of structure alterations, preparation of polished sections and bringing out the microstructure is of paramount importance. In this work, specimens were mechanically polished. Microstructure was revealed by electroetching using electrolytes and processes proposed by the All-Union Institute of Aviation Materials (VIAM) (see table)

Reagent composition	Etching process, current strength, and etching time	Microstructure
10 g $(\text{NH}_4)_2\text{SO}_4$ 10 g citric acid	0.1-0.2 a/cm <sup>2</sup> 5-6 seconds	strengthened γ'-phase
water 1 m <sup>3</sup>	0.1-0.2 a/cm <sup>2</sup> 120-180 seconds	cellular structure
10 % NaOH + H <sub>2</sub> O <sub>2</sub>	0.1-0.2 a/cm <sup>2</sup>	carbide phase

Results of investigation. Study of the structure state of samples subjected to thermal cycling (samples were heat treated by V. I. Borisov).

Samples were subjected to thermal cycling with air cooling after 1, 75 and 400 cycles and with water cooling after 1, 75 and 280 cycles.

No noticeable change of the carbide constituent was revealed nor was there any essential change noted between structure of the center and that of the area adjacent to the surface of polished sections (Figs. 1, 2). For comparison, Figs. 1 and 2 show the microstructure of samples quenched in water after one and 280 cycles. Thermal cycling of samples with air cooling from a fan does not lead to formation of cracks even after 400 cycles. Apparently, stresses forming under such conditions

are insufficient for crack formation. Testing of samples under more rigid conditions causes microcracks to appear even after 75 cycles and the formation of a large number of visible cracks is noted after 280 cycles. Microscopic investigations show that not all cracks emerge at the surface. A portion of the cracks is located at a depth of 0.1-0.2 mm from the surface (Fig. 1a). It is possible at this depth that stresses, forming in connection with varying rate of heating and cooling of the surface and internal areas of the sample, are maximum.

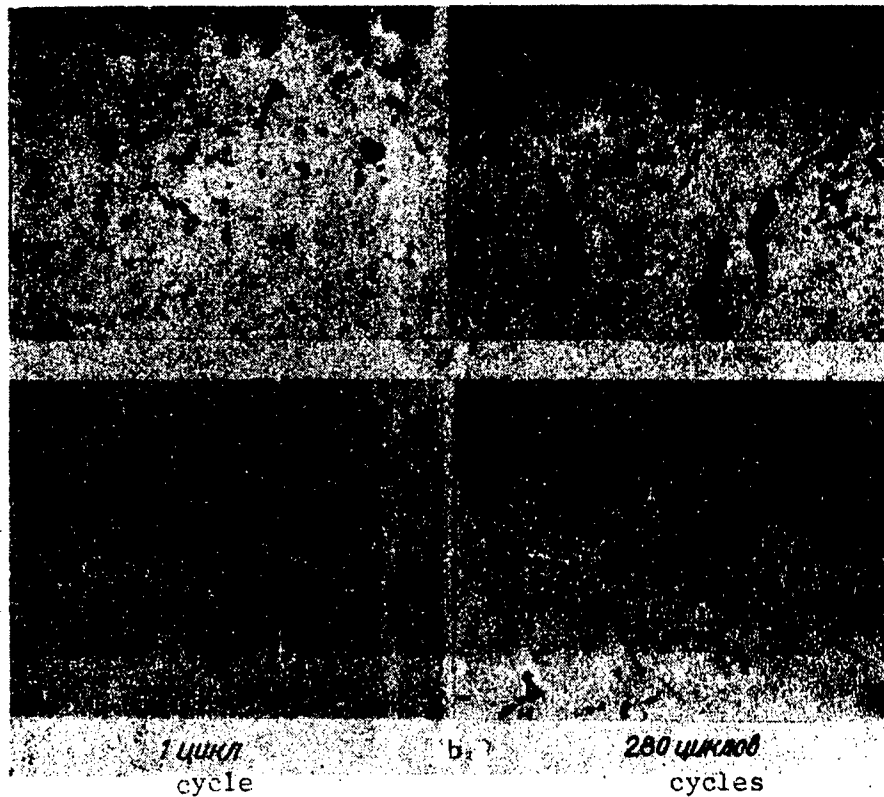


Fig. 1. Microstructure of thermally fatigued samples, water quenched and carbide phase etched, after one cycle (left) and 280 cycles (right): a--surface layers (70X); b--internal layers (100X).

Microstructure study of the  $\gamma'$ -phase in the samples showed that increasing the number of cycles and changing the conditions of cycling does not significantly change shape and position of the  $\gamma'$ -phase (Fig. 2a, b). Slight coalescence of the  $\gamma'$ -phase within the grains and more vigorous coalescence in the grain boundaries is observed only at a large number of

thermal cycles which is verified by electron microscopy (Fig. 2b). Apparently, the more predominant factor in coalescence of carbides and the  $\gamma'$ -phase is not the number of cycles but the temperature and holding time at the maximum cycle temperature.

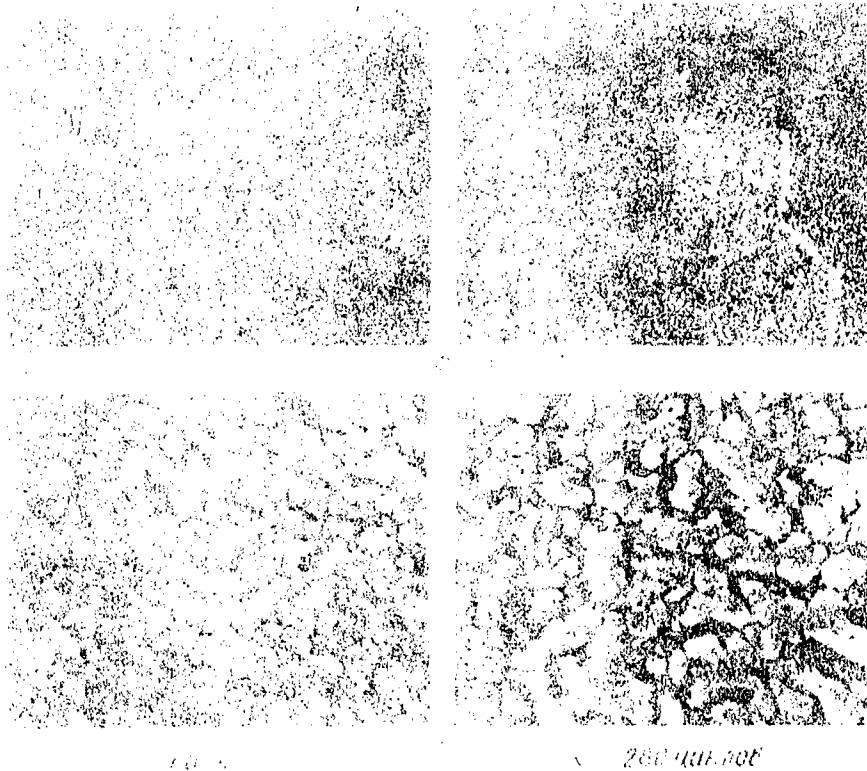


Fig. 2. Microstructure of thermally fatigued samples, water quenched and  $\gamma'$ -phase etched, after one cycle (left) and 280 cycles (right): a--surface layers (70X); b--internal layers (3000X).

Effect of unsteady heating on structure of surface layers and internal zones of nozzle vanes.

Microstructure and electron microscope investigations of cast and heat treated vanes indicate essential distinctions in their structure. In a heat treated vane there is observed considerable dissolution of carbides as compared with cast vanes. As is known, chromium carbides and binary carbides, being disposed primarily in the grain boundaries, embrittle the alloy. Processes of carbide formation in grain boundaries promote depletion of the  $\delta'$ -phase by alloying elements, which alleviates coalescence of the  $\gamma'$ -phase.

Structure changes in nozzle vanes, having passed standing tests after a varying number of thermal cycles, were initially studied on vanes of various melts. Apparently, in connection with the fact that vanes were of various shapes, varying thermal cycling from different heats did not reveal an association between number of cycles and formation of cracks. Thus, from eight vanes, after 70, 100, 162, 192, 275, 300, 500 and 650 cycles, deep cracks were observed on the leading edge after 70 and 275 cycles.

Microstructure investigations of surface layers and internal regions of vanes with cracks on the leading edge after etching the carbides and  $\gamma'$ -phase showed that no particular change in location of the  $\gamma'$ -phase and carbides, as compared with a heat treated vane, is observed. The  $\gamma'$ -phase is uniformly distributed in the matrix of the solid solution. Investigations of the geometry of crack development shows that that cracks are situated in the grain boundaries (Fig. 3b).

A concrete result of structure changes in surface layers of vanes having cracks was obtained in a study of the surface layers of deeply etched samples (Fig. 3a and 3b).

From Fig. 3 it is clear that a brief etching of a section of a vane in the cracked region (from the leading edge) did not reveal any essential difference in the structure state of the surface and internal sections of the sample. Increasing the etching time from two to five minutes revealed a unique cellular structure in the surface layers (Fig. 3b). This cellular structure is observed in the surface layers of the leading edges of vanes which had undergone thermal fatigue tests and cracked after 70 and 275 cycles (Figs. 3b, 4b, and 5b). Depth of surface layer with the cellular structure was 0.1-0.2 mm for vanes after 70 cycles and 1-2 mm for vanes after 275 cycles. It must be noted that the cellular structure is revealed not only in the region of cracking but on a considerable portion of the leading-edge surface, and in many vanes is present in the entire leading edge (Fig. 4).

The most pronounced cellular structure is revealed in surface zones of a vane. At a certain depth from the surface, the  $\gamma'$ -phase is ingrained on the light background of the cellular structure and the amount of  $\gamma'$ -phase present gradually increases where at a depth of 0.1-0.2 mm the cellular structure completely disappears. Only the  $\gamma'$ -phase is evenly interdispersed in the matrix of the solid solution (Fig. 5a and 5b). Cell dimensions change from 30 millimicrons on the surface to 5 millimicrons in deeper layers. The cellular structure has preferred orientation within the boundaries of each grain (Figs. 3b and 5b). Transition from one grain to another is accompanied by change of orientation and shape of individual cells (Fig. 6).

In a vane after 500 cycles, in which there are no thermal fatigue cracks, the cellular structure is not present. Comparison of vanes after 70, 275, and 500 cycles shows that in a vane



Fig. 3. Microstructure of vane after 275 cycles of testing in the cracked region,  $\delta'$ -phase etched: a--etching time-25 seconds; b--etching time-100 seconds (70X).

after 500 cycles, there is noticeable coalescence of the  $\gamma'$ -phase both inside the grains and in the grain boundaries.

In one vane from the investigated alloy, a deep crack in the trailing edge was observed. Microscopic investigation of this vane showed that the cellular structure was not only close to the cracks but on the entire trailing edge of the vane (Fig. 4a),

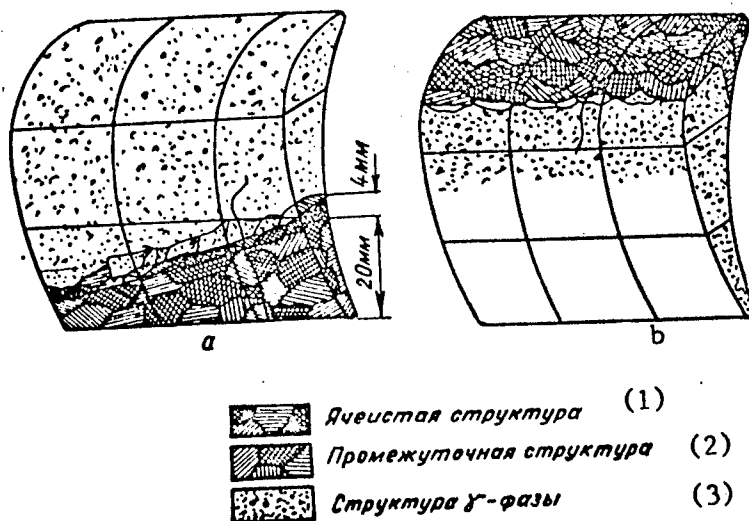


Fig. 4. Illustration of the distribution of cellular, intermediate, and  $\delta'$ -phase structures in: a-- a vane with a crack on the trailing edge, b--a vane after 275 cycles. 1--cellular structure, 2--intermediate structure, and 3--structure of the  $\gamma'$ -phase.

The lack of an evident relationship between number of cycles and formation of cracks in vanes of the first batch made it necessary to conduct a similar investigation of vanes from one heat. This series of vanes were investigated after 50, 75, 100, 150, 240, 350, and 480 cycles. It turned out that there is a definite relationship between number of cycles and formation of cracks.

In all vanes of this heat, starting at 100 cycles and above, cracks were observed in the leading edge. Microstructure studies showed that, in vanes with cracks, the cellular structure will be in a narrow region in the leading edge. The width of this region varies from vane to vane and in the same vanes varies from 0.1 to 6 mm.

It was interesting to note that in a vane after 350 cycles, the cellular structure is found on a restricted section in the region of the leading edge where the cracks are also observed.

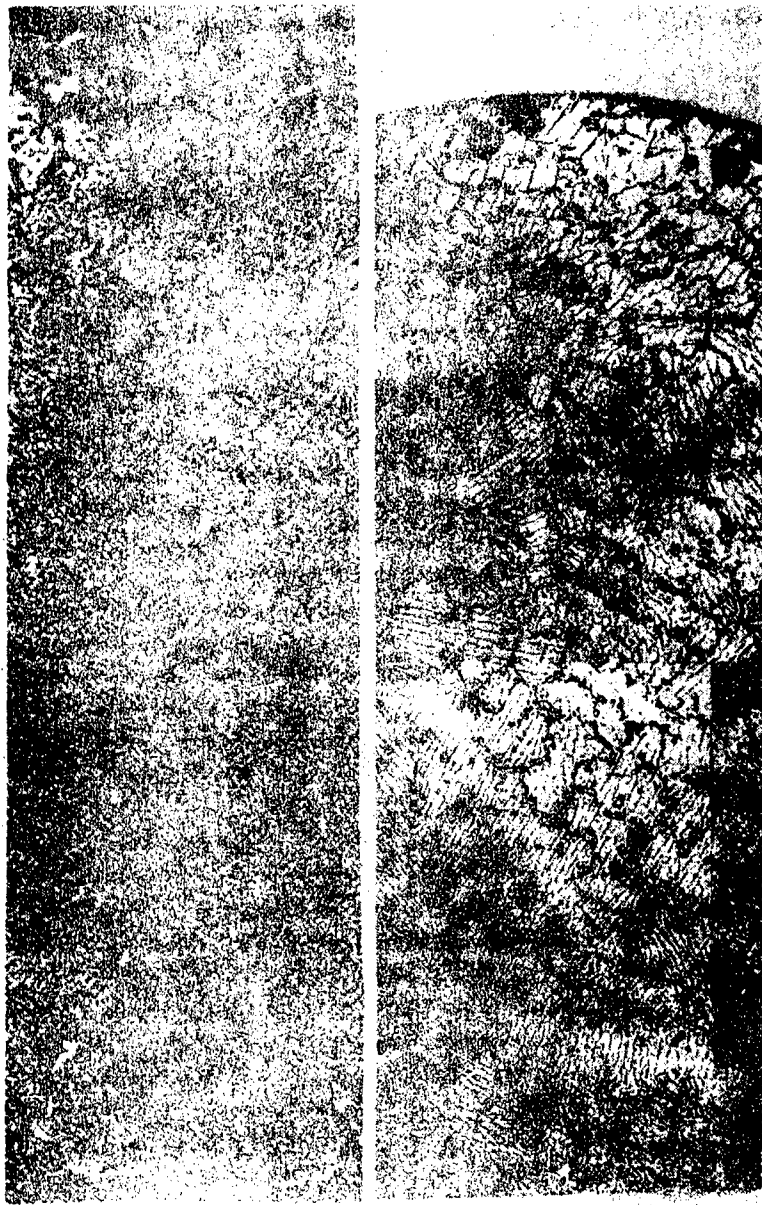


Fig. 5. Cellular structure in cross section of vane leading edge: a--after 70 cycles (650X); b--after 275 cycles (70X).

The existence of the cellular structure in the surface zone was established also in a vane made from an alloy of similar composition which cracked along the leading edge.

### Discussion of results

The microstructure of vanes in the cracked region shows that fracture occurs primarily in the grain boundaries (Fig 3b).

In individual cases it was possible to establish that the initial stages of fracture are a loosening of the structure being transformed into microcracks along the grain boundaries of the cellular structure. Apparently, as a result of cyclic loading at these points, defects are accumulated and, at specific stages, lead to the formation of microcracks (Fig. 5a). These observations agreed with x-ray studies of work [4] in which the authors arrive at the conclusion that, as a result of cyclic thermal stresses over a period of time, preceding the appearance of cracks, plastic deformation is intensely accumulated (decrease dimensions of blocks which corresponds to an increase of dislocation density).

#### 1. Effect of thermal cycling on formation of cellular structure.

For explanation of the conditions of formation of the cellular structure, alloy samples, after normal heat treating, were subjected to repeated heating at various temperatures, held at temperature for different periods of time, and cooled in water or air, or furnace cooled. It turned out that the cellular structure appears when alloys are heated at 1180-1200C. Further increase of temperature accelerates this process. After eight hours at 1180 C, individual areas with the cellular structure are noticed. Increase of temperature to 1200 C promotes clear manifestation of the cellular structure within 15 minutes, but at 1300 C only 5-10 minutes was required. Prerequisite for stabilization of the cellular structure appears to be the condition of cooling. The faster the cooling rate, the more clearly this structure is revealed. Slow furnace cooling does not promote formation of the cellular structure even after heating to high temperatures (1250-1300 C). Analysis of the microstructure and results of x-ray studies, after various forms of heat treatment, form a basis to explain when and why the cellular structure is formed. At the present stage of investigation, these conditions proposed by us are: in heating to 1180-1200 C and above causes dissolution of the excess phases (carbides and  $\gamma'$ -phase) in the matrix of the solid solution. The higher the heating temperature and longer the holding time at temperature, the faster these processes will proceed. During subsequent cooling the  $\gamma'$ -phase precipitates out and, in this instance, precipitation cannot be retarded even by water quenching. Cooling rate has a significant effect on degree of dispersity of the

$\gamma'$ -phase. During rapid cooling, a highly dispersed  $\gamma'$ -phase will be formed which is almost invisible at low and medium magnifications, but is satisfactorily resolved at high magnifications. Its presence is easily revealed by the presence of a black precipitate which can be removed from the surface of the polished section (x-ray diffraction analysis of the black precipitate confirmed existence of the  $\gamma'$ -phase). Thus, the high degree of dispersity of the  $\gamma'$ -phase is, apparently, the decisive condition for manifestation of the cellular structure. Coalescence of the  $\gamma'$ -phase occurs during slow cooling and the cellular structure does not form. Based on these observations, it was possible to assume that the cellular structure can be annihilated by additional heating to a temperature that will ensure coalescence of the  $\gamma'$ -phase. To check this, a sample with the cellular structure was vacuum heated at 1100 C for five hours. After repolishing and deep etching, the structure shown in Fig. 6b was revealed. Thus, as is possible to see, coarsening of the  $\gamma'$ -phase took place and at the same time the cellular structure disappeared. Heating to higher temperatures (1200 C) with subsequent rapid cooling again leads to formation of the cellular structure. Thus, at certain conditions, this process can be completely reversed. Naturally there is the question if the cellular is really annihilated; is this only an apparent effect associated with peculiarities of etching? At present, it is only possible to make assumptions, but to us it seems that they will be better founded after additional experimentation. Apparently, in actual conditions of nozzle vane operation, when there are simultaneous changes of chemical composition of the surface layers, temperature and time conditions for formation of cellular structure can change. However, at present there are no data on this problem.

## 2. Nature of the cellular structure

In microstructure analysis appears the question on the fact that there is a cellular structure and is it a result of etching? In the process of investigation many samples were subjected to repeated polishing and etching. In all cases the revealed microstructure was always the same. In addition, as one may see from Fig. 5a, in the surface layers, only the cellular structure is observed. The transition to deeper layers shows that the finely dispersed  $\gamma'$ -phase is revealed on the background of the cellular structure. Internal sections of the polished section always contained precipitated particles of carbides and the  $\gamma'$ -phase. This observation leads to the conclusion that the cellular structure may be associated with a causal effect of etching.

Some authors associate the formation of a similar type structure with formation of oxidized films and their subsequent

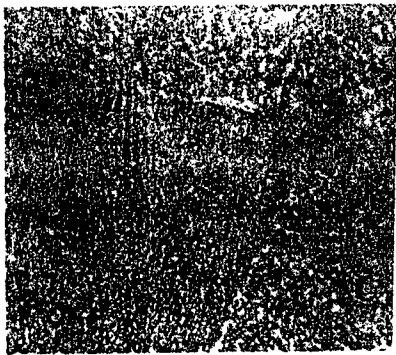
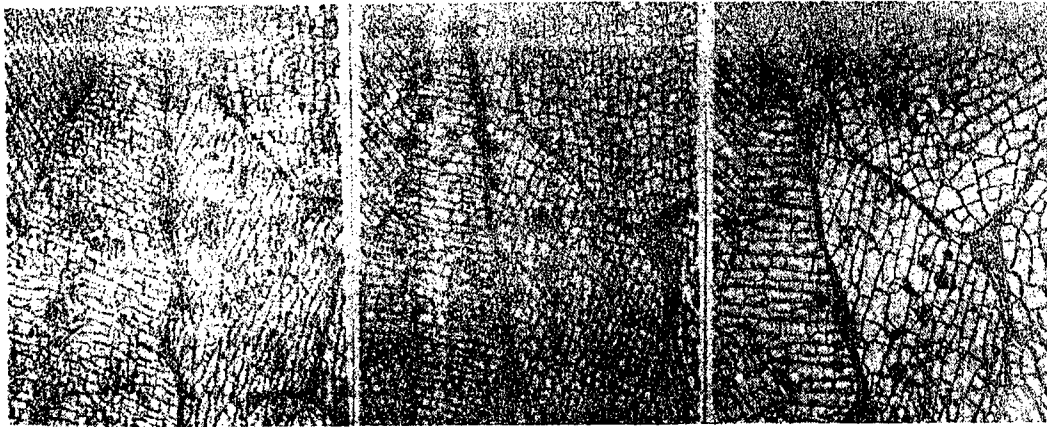


Fig. 6. Reproducibility of cellular structure: a--repeated deep etching into  $\delta'$ -phase of a sample quenched from 1200 C after holding for 0.6 kiloseconds (70X); b--same sample after holding at 1100 C for five hours (600X).

cracking in crystal planes peculiar to the metal under the oxide film. Thus, in work [57] the film method of etching was used for metallographic study of the substrate of silicon electric steels. As a result of using this special form of etching, a similar structure was also observed in research on ferritic magnesium iron [67].

Special tests were carried out to explain the nature of the cellular structure. Samples with a cellular structure were subjected to repolishing and etching many times. In Fig. 6a, microphotographs are shown of the same polished section after repeated polishings. As evident, in all cases the nature of cell orientation is preserved, although cell size is changed. Preservation of cell orientation after repolishing in the confines of one grain and its change in the transition to another grain serves as an indication that the cellular structure reflects crystallographic orientation of the grains. However, change of cell size places identity of structure and substrate in doubt.

Therefore, it is possible to assume that the cellular structure in this case is a result of film etching of the metal which is in a specific structure state. This structure, as evident from metallographic investigations (Fig. 5a) can be associated with the varying degree of dispersity and quantity of the  $\delta'$ -phase in the surface sections and internal regions of the metal. However, it is necessary to take into account

the effect of change of chemical composition of surface layers as a result of interaction of vanes with corrosive gas flow.

### 3. Cellular structure and formation of cracks.

We attempted to relate formation of the cellular structure and formation of microcracks in the surface layers of vanes. Actually, if the cellular structure characterizes a change of structure state of vane surface layers, it can be deduced that the surface layers possess less resistance to thermal fatigue and are the most probable sites for formation and development of microcracks. However, it is known that thermal cycling to 1000 C forms cracks although there is no cellular structure. Upon increasing the cycling temperature, the formation of cracks proceeds much faster. At these conditions (heating to 1180 C) the cellular structure is revealed.

While the only assumption that can be made is that formation of the cellular structure can accelerate microcracking, which can lead to failure of nozzle vanes. The physical nature of this association must be further studied. It will be necessary to give attention to the fact that appearance of the cellular structure in thin surface layers after stand tests may be connected with local overheating.

### BIBLIOGRAPHY

1. I. A. Vladimirov, Trudy KVIAU (Works of KVIAU), No 93, Kiev, 1961.
2. E. Glenny, T. A. Taylor, Jour. of the Inst. of Metals, No 7, pp 449-462, 1960.
3. P. G. Kolomytsev, A. A. Samgin, A. Ye. Snetkov, Metallovedeniye i Termicheskaya Obrabotka Metallov (Physical Metallurgy and Heat Treatment of Metals), No 9, pp 7-12, 1960.
4. A. P. Glazov, L. I. Lysak, L. V. Tikhonov, M. S. Khazanov, (see pp 111-120 in this book),
5. S. A. Shvets, Fizika Metallov i Metallovedeniye (Metal Physics and Metals Science), Vol 13, No 2, 1962.
6. A. I. Yatsenko, Metallovedeniye i Termicheskaya Obrabotka Metallov, No 12, 1959.

6368  
CSO: 1879-D/PE

INVESTIGATION OF CRYSTAL STRUCTURE CHANGE  
DURING THERMAL FATIGUE OF ALLOY ZhS-6K

[Following is a translation of an article by A. P. Glazov, L. I. Lysak, L. V. Tikhonov, and M. S. Khasanov] in the Russian-language book Voprosy Fiziki Metallov i Metallovedeniya (Problems of Metal Physics and Metals Science), Collection of Scientific Works of the Institute of Metal Physics, No 17, Kiev, 1963, Academy of Sciences Ukrainian SSR, pp 111-119.]

Thermal fatigue is one of the basic factors leading to fracture of nozzle vanes of gas turbine engines. Thermal stresses occurring during stopping and starting of an engine and during switch-over from one mode of operation to another sharply reduces the service life of vanes.

Cracks formed in the process of thermal cycling usually appear in surface layers of a vane and upon further operation rapidly lead to vane fracture.

At present it is generally accepted that the main processes occurring in unsteady thermal actions are thermal stresses. These stresses which exist all the time are functions of the temperature gradient  $\Delta T$  and, as a rule, are greatest in the surface layers and therefore cause structure changes in these layers.]

One may consider that in the process of cyclic heat treatment there occurs an accumulation of elastic macro-strain (stresses of the first order) which brings about the formation of cracks. Apparently, change of phase composition has much significance, as this occurs in the surface layers under the effect of thermal stresses [17]. There are data on the fact that thermal cycling activates the aging process as compared with its isothermal nature at the highest temperature of the cycle [2, 37]. The variation in the process of cyclic heat

treatment on dislocation distribution in the surface layers /47 also is important. It should be noted that the shape and surface condition of a part effects resistance to thermal fatigue as does the parameters of the temperature cycle /5, 67. Oxidation of the surface layer also plays an essential role.

In spite of a large number of works on the study of thermal fatigue of heat-resisting alloys and parts, the problem is still far from being adequately understood.

Many researchers studied thermal fatigue of various materials which were quite different in shape from vanes and also under conditions quite different from actual conditions.

Nozzle vanes of gas turbines were investigated in this present work by x-ray diffraction at conditions approaching actual operating conditions (temperature, composition of medium-combustion products of diesel fuel, gas flow-rate, etc.).

Inasmuch as a crack is obviously the result of the same structure changes which accumulate in surface layers of vanes during thermal cycling, it was necessary to conduct x-ray investigations of vane surface layers with respect to the number of cycles before and after cracking.

It was also interesting to investigate changes of surface condition of vanes in the process of machining.

The presented problems were solved in our work by means of investigating the state of the matrix solid solution.

Several cast vanes made of heat-resisting alloy ZhS-6K were produced. Heat treating vanes was done as follows: four hours at 1200 C with subsequent air cooling. In order to explain the effect of machining on structure of the surface layer, three forms of vanes were investigated: unmachined, rough machined, polished. Polished vanes were subjected to thermal cycling on a special unit under two variants: 1) 400°-30 seconds; 500°-30 sec; 800°-60 sec; 400°; b) 400°-30 sec; 700°-30 sec; 950°-60 sec; 400°. *Page 20*

#### Method of investigation

X-ray investigation of the  $\gamma$ -solid solution of vane surface layers was done in an ionization chamber URS-50I with automatic recording of radiation scattering. Rotating speed of scintillation counter was 0.415 milliradians/sec and rate of movement of diagram strip of recording instrument was 0.445 mm/sec. Lines (111), (220), and (222) of the  $\gamma$ -solid solution were recorded using Co-K $\alpha$  radiation.

In the investigation vanes were placed on the largest stand of the URS-50I unit and not rotated in the plane of the polished section. In photographing slices of vane samples they were rotated in the plane of the polished section at 6.28 rad/sec. As a rule the surface layers were studied but in some cases deeper areas were studied by means of etching.

The change of  $\gamma$ -phase lattice parameter was determined by the change of the angle of reflection of interference lines. Determination of the dimensions of the regions of coherent scattering and magnitude of micro-distortions was done according to methods described in works [7, 87].

### Results of investigation and their discussion

Results of measuring the lattice parameter of the  $\gamma$ -phase in the region of possible crack formation (middle of leading edge on concave side) in vanes are presented in Fig. 1.

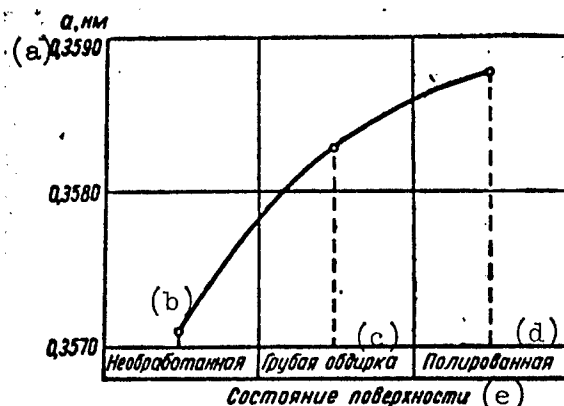


Fig. 1. Curve of the change of lattice parameter of the  $\gamma$ -phase on surface of vane to stage of mechanical working: a--lattice parameter a, nm; b--unmachined; c--deep roughing; d--polishing; e--distance from surface.

From Fig. 1 it is evident that machine leads to some increase in lattice parameter. These results are explained in that, during casting and heat treating, layers are formed on the surface which differ in composition from the ZnS-6K alloy, and upon further roughing and polishing these layers are removed. This explanation is verified by a change in the lattice parameter after etching of unmachined and polished vanes at various depths. For example, when etching and unmachined vane the following results are obtained:

depth of etching, mm	0.00	0.05	0.10
lattice parameter of of $\gamma$ -phase, nm	0.3571	0.3581	0.3589

Results of x-ray examination of the surface layer of a polished vane with respect to depth of etching are shown in Fig. 2. As one can see, in etching the finished surface of a vane, the  $\gamma$ -phase parameter remains almost unchanged. Thus,

roughing and polished of the surface completely removes the layer of variable composition which is formed during pouring (casting) and heat treatment of the vane.

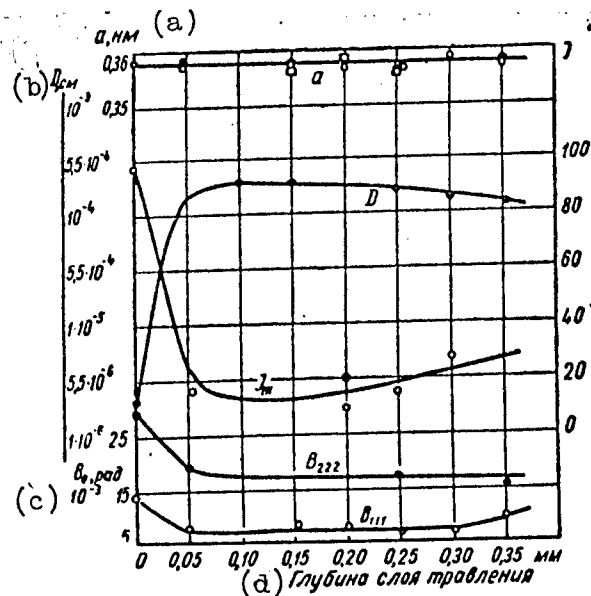


Fig. 2. Curves of the change in line widths ( $B_{111}$  and  $B_{222}$ ), integral intensity of line  $111$  ( $I_{111}$ ), lattice parameter, and size of the region of coherent scattering of the  $\delta$ -phase according to depth of the surface layer in a vane: a--lattice parameter  $a$ , nm; b--depth  $D$ , cm; c-- $B_{\theta}$ ; d--depth of etched layer.

From Fig. 2 one may conclude that the thickness and structure of the cold-worked surface layer, which is important in this case, have a decided effect on resistance to thermal fatigue [57]. These data obtained in filming the concave region of the vane along the leading edge show that the width of lines (111) and (222) and the intensity of line (111) are changed up to a depth of 0.1 mm from the vane surface, i. e. the depth of the cold-worked layer is approximately 0.0-0.1 mm deep. Size of the region of coherent scattering and magnitude of micro-distortions on the surface of the vane were determined from widths of lines (111) and (222) and found to be  $\Delta a/a \approx 2.7 \times 10^{-3}$  and  $D \approx 3 \times 10^{-6}$  cm respectively. From modeled presentations developed in [9-11] it follows that distribution of dislocations on the surface of a finished vane is random. Even at a depth of approximately 0.05 mm microdeformations are practically zero and the size of the blocks of coherent scattering exceed  $1 \times 10^{-4}$  cm. Deeper in the vanes the size of these blocks does not change.

A vane was similarly investigated at 650 cycles (without cracks) according to mode 1 (page 14). Results of this study are presented in Fig. 3. X-ray photographs were taken at four regions of the vane surface: 1) the region of the leading edge on the concave side (parameters-- $a_1$ ,  $I_{111}$ , and  $D--\circ$ ; 2) region of the leading edge on concave side (parameters-- $a_2$ ,  $I_{111}$ , and  $D--\bullet$ ; 3) concave region in center section (parameter-- $a_3$ ,  $I_{111}$ , and  $D--\square$ ; 4) back side in center (parameter-- $a_4$ ,  $I_{111}$ , and  $D--\circ$ ).

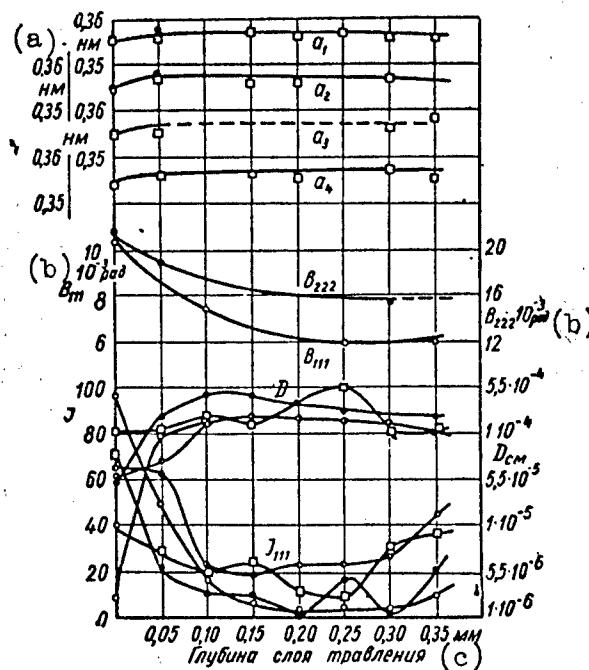


Fig. 3. Characteristics of crystal structure of vane surface layer after 650 cycles: a--nm, b--radians, c--depth of etched layer

Lines widths on graph are for those regions on the leading edge, concave side.

From the presented data it is clear that in the process of thermal cycling a layer of variable composition is formed in the surface layer (with diminished parameter of the  $\delta$ -phase) with a thickness on the order of 0.05 mm. In the region of the same thickness there occurs a greater change in the intensity of line (111). At a depth of 0.05-0.10 mm, lines (111) and (222) are the strongest.

Thus, all structure changes, accumulated as the result of thermal cycling, are concentrated primarily in the fine surface layer with a thickness of 0.05-0.10 mm.

Judging by the intensity of lines (111) it is interesting to note that the size of the regions of coherent scattering is smallest ( $\sim 10^{-6}$  cm) in the zone where cracks had been previously noted (on the leading edge, concave side). The same order of block dimensions ( $\sim 3 \times 10^{-6}$  cm) gives an estimate as to widths of lines (111) and (222). In other zones the size of the regions of coherent scattering are much larger.

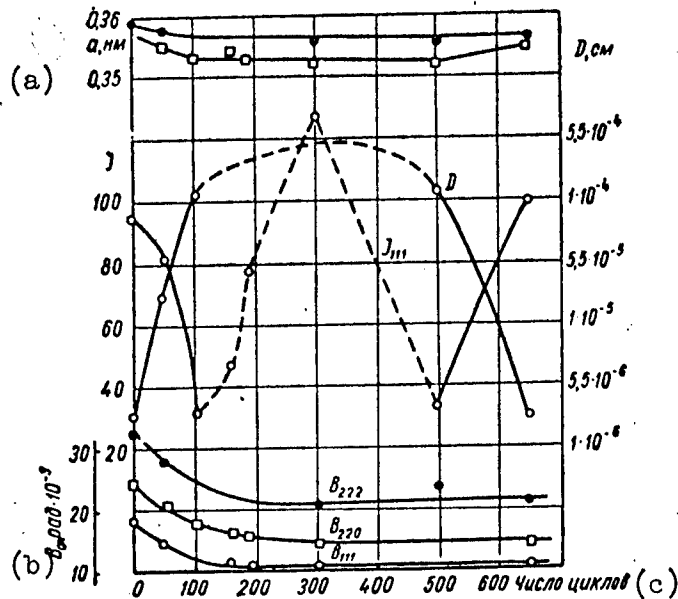


Fig. 4. Effect of the number of thermal cycles on characteristics of the crystal structure of the  $\delta$ -phase (variant 1): a--lattice parameter-a, nm; b--radians; c--number of cycles.

In spite of the small size of the blocks in the zone of the leading edge (it is the same as in the initial unmachined vane), microdeformations of the  $\delta$ -phase lattice are not observed. This fact can be explained principally by the varying distributions of dislocations in the surface layers of the original vane and vanes subjected to 650 cycles. The produced result fully agrees with the result of work [47].

Fig. 4 shows data obtained on vanes with respect to number of cycles (0 to 650) according to variant 1. None of the vanes of this batch had any cracks. An x-ray photograph was taken of the surface of an unsectioned vane in the zone of the leading edge, concave side.

From the presented data one can see that at approximately 100 cycles the interference lines are almost completely nonexistent which indicates removal of lattice microdeformations and increasing of the regions of coherent scattering. The change of lattice parameter is completed at 100 cycles on the

surface of the vanes (black circle--at line (111), square--at line (220)). The intensity of line (111) up to 100 thermal cycles is steadily diminished indicating an increase in the size of the regions of coherent scattering from  $3 \times 10^{-6}$  to  $1 \times 10^{-4}$  cm. In the interval between 100 and 500 cycles lines (111) become spotted and it is impossible to measure their intensity. However, this fact is witnessed by the fact that after many cycles the grains and blocks in the vanes are coarser. At 650 cycles the lines again become solid and their intensity is increased. This phenomenon corresponds to decreasing size of regions of coherent scattering (by calculation this is  $3 \times 10^{-6}$  cm).

Comparing all the above-mentioned data on change of lattice parameter, it is possible to arrive at a conclusion on the fact that change of lattice parameter on the surfaces of vanes during increase in number of cycles is explained by the composition alteration of the surface layer, but not by an increase of elastic deformation as manifested by stresses of the first order.

Thus, elastic macrodeformation in the process of thermal cycling is not accumulated. At the same time, the nature of change in the number of cycles of the elastic microdeformations of the lattice and the size of the regions of coherent scattering indicates that if in the initial stages of thermal cycling (100-150 cycles) temperature plays a more predominant role (removal of microdeformations and increase of block size, i. e., decrease of dislocation density), then at a higher number of thermal cycles the danger zone for appearance of cracks will be reached (500-650 cycles in the given case) and plastic strain is accumulated (increase of dislocation density). In this instance dislocations are not randomly dispersed, but are distributed in such a way that the elastic lattice energy is less than in a chaotic distribution of dislocations (an example of such a distribution is grouping of dislocations in the shape of a vertical wall and their association).

On the basis of these premises it one may consider that disturbance of continuity of a solid material (crack formation) occurs not as a result of accumulation of elastic macrodeformation in the surface layer, but because of accumulated alterations in the fine crystal structure by which the material loses its ability to withstand unsteady thermal stresses.

It must be noted that the above-described regularity of structure changes, depending upon number of thermal cycles, were confirmed by an investigation of other batches of vanes which were tested according to mode 2. Results of these investigations are presented in Fig. 5. The vanes of this batch began cracking at 100 cycles (in Fig. 5., vanes with cracks are marked below with arrows). As in the preceding case, lines are completely narrowed at 100 cycles. At this point the change of lattice parameter of the  $\gamma$ -phase is completed.

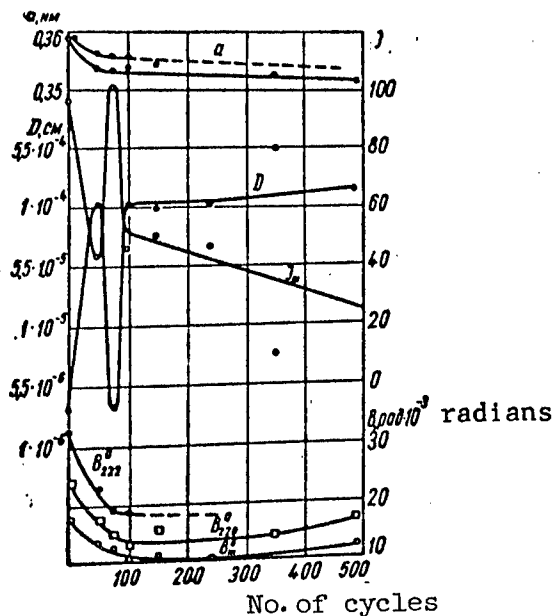


Fig. 5. Effect of number of thermal cycles on properties of the  $\gamma$ -phase crystal structure (variant 2).

Size of blocks in the danger zone is increased at first (at 50 cycles it is close to  $1 \times 10^{-3}$  mm and then sharply decreases to the point where at 75 cycles the size is approximately  $3 \times 10^{-5}$  mm), after which follows crack formation. After crack formation blocks in regions adjacent to the cracks become larger indicating the predominant effect of temperature in forming of structure; the fact of breaking up of blocks before disturbing material structure agrees with the results of work [12] in which thermal fatigue of pure copper was studied.

More detailed information on factors which determine thermal fatigue can be obtained by studying phase changes in the surface layer and a more local study of crystal structure in relation to number of thermal cycles.

### CONCLUSIONS

The change of imperfections of a crystal structure and the parameter of the  $\gamma$ -phase on the surfaces of alloy ZhS-6K nozzle vanes was studied with respect to the number of thermal cycles and also the change of these properties in layers at varying distances from the vane surfaces. Investigation was conducted on vanes in the zone of most probably crack formation.

Results showed that significant changes of structure during thermal cycling occur only in the surface layers at depths of 0.05-0.10 mm. A noticeable change of microstresses and lattice parameter of the  $\gamma$ -phase occurs at a relatively small number of thermal cycles (approximately 100). Upon further increase in number of thermal cycles these properties do not change before or after formation of cracks.

Upon increase in number of thermal cycles the size of the regions of coherent scattering is increased at first (from  $3 \times 10^{-6}$  cm in the initial state to an order of  $10^{-3}$  mm), and then decreases to a magnitude of approximately  $3 \times 10^{-6}$  after which cracks appear.

In vanes with cracks, dimension of the regions of coherent scattering is  $10^{-3}$  cm.

The obtained data shows that during thermal cycling of vanes there is no noticeable accumulation of elastic macro- and micro-deformation in the surface layers as compared with the initial state. At the same time, before formation of a crack, an intense accumulation of plastic strain is observed, accompanied by an increase in dislocation density. One must note that in the surface layers of the initial vane and in a vane, approaching a condition of thermal fatigue, various distributions of dislocations are observed.

### CONCLUSIONS

1. G. V. Kurganov, Yu. L. Sultina, Metallovedeniye i Obrabotka Metallov (Metallography and Metal Processing), No 10, 1958, p 23.
2. V. S. Yermakov, Metallovedeniye i Termicheskaya Obrabotka Metallov (Metallography and Heat Treatment of Metals), No 4, p 14, 1959.
3. K. V. Savitskiy, Yu. I. Paskal', and T. I. Gvozdeva, Izvestiya Vysshikh Uchebnykh Zavedeniy, Fizika (News of the Higher Educational Institutions, Physics), No 6, p 109, 1960.
4. I. A. Vladimirov, Issledovaniye Termostoykosti Turbinnykh Lopatok (Investigation of the Heat Resistance of Turbine Blades), KVIAU, Kiev, 1961.
5. Ya. B. Fridman, and V. I. Yegorov, Metallovedeniye i Termicheskaya Obrabotka Metallov, No 7, p 27, 1960.
6. G. P. Lazarev, Izvestiya VUZov, Tsvetnaya Metallurgiya (News of the Higher Educational Institutions, Nonferrous Metallurgy), No 6, p 149, 1960.
7. L. I. Lysak, Voprosy Fiziki Metallov i Metallovedeniya (Problems of Metal Physics and Metal Science), No 6, p 49, 1955.
8. L. I. Lysak and L. V. Tikhonov, Fizika Metallov i Metallovedeniye (Metal Physics and Physical Metallurgy), Vol 7, No 5, p 758, 1959.
9. D. Vil'yamson and R. Smollmen, Problemy Sovremennoy Fiziki (Problems of Modern Physics), No 9, 1957.
10. K. P. Ryaboshapka and L. V. Tikhonov, Fizika Metallov i Metallovedeniye, Vol 11, No 4, p 489, 1961.
11. K. P. Ryaboshapka, and L. V. Tikhonov, Fizika Metallov i Metallovedeniye, Vol 12, No 1, p 3, 1961.
12. L. M. Rybakova and S. Z. Yermol'chik, Fizika Metallov i Metallovedeniye, Vol 9, No 5, p 734, 1960.

6368

CSO: 1879-D/PE

EFFECT OF UNSTEADY HEATING ON CHANGE OF  
MAGNETIC AND ELECTRICAL PROPERTIES OF  
ALLOY ZhS-6K

[Following is a translation of an article by V. I. Borisova, I. Ya. Dekhtyar, E. G. Madatova, V. S. Mikhalenkov, R. G. Fedchenko, and M. S. Khazanov in the Russian-language book Voprosy Fiziki Metallov i Metallovedeniya (Problems of Metal Physics and Metal Science), Collection of Scientific Works of the Institute of Metal Physics, No 17, Kiev, 1963, Academy of Sciences Ukrainian SSR, pp 120-131.]

[From published works on the problem of thermal fatigue no satisfactory theory on the phenomenon has been developed.] This is explained, on one hand, by the complexity of the problem and the large number of factors to be considered, and on the other hand, by the fact that there is no detailed explanation of the basic physical factors, change of physical factors, and change of phase states in the process of thermal fatigue.

In connection with this [it is quite important that this problem be studied in order to devise new methods of investigation which are sensitive to phase and structure changes which occur in the process of thermal cycling of heat-resisting materials.

One of these sensitive methods, used in this work, is that of paramagnetic susceptibility. In conjunction with other methods, being responsive to changes of both structure and phase states, paramagnetic susceptibility responds only to change of phase state of an alloy in the process of cyclic treatment. This should make it possible to solve the problem concerning the interrelationships in structure and phase as to whether they occur consecutively or simultaneously and to what degree they are developed in the process of thermal fatigue. The following methods were also used in this work: /

1100 1100 1100  
measurement of hot hardness, electrical resistance, deformation, and measurement of surface electrical resistance using eddy current loss values. 1100

Change of hardness and sample shape during thermal cycling of alloy ZhS-6K.

One of the important problems of modern physical metallurgy is the study of metal behavior under cyclic loads caused by thermal cycling. Thermal stresses are set up in a part when it is heated and cooled at a certain rate. The multiplying effect of thermal stresses cause the formation of cracks and fracture of the metal. This phenomenon is analogous with the action of variable mechanical loads on a material and is called thermal fatigue. In a number of instances the phenomenon of thermal fatigue causes failure of a part by means of shape or dimension change.

Formation of thermal stresses is explained by non-uniform state of various points of parts and is associated with the entire combination of solid state physical and mechanical properties. In heating and cooling at a specific rate the temperature at different areas of the surface will differ. Thus, there will be a fully defined temperature distribution in the cross section of a body for a given period of time. The magnitude of the temperature gradient depends on heat capacity and thermal conductivity of the material and rate of heating and cooling.

In nonuniform heating the field of free expansion of the hotter sections will prevent thermal expansion of the cooler sections. As a result, stresses will form. If the formed stresses exceed the yield point at a given temperature, then plastic deformation of individual sections of the material will take place. These stresses will then lead to the formation of cracks. However, the problem of what takes place prior to crack formation remains unstudied. Since the magnitude of thermal stresses is of such a significant degree, then in the course of heating and cooling of the initial cycles certain irreversible processes in the sample take place.

The present work is devoted to a study of the action of thermal stresses on deformation and hardness of alloy ZhS-6K in the process of thermal cycling.

The study of ZhS-6K deformation was conducted on cylindrical samples with a diameter of 3 mm and length of 100 mm. Shape of a sample for a study of the dimension changes plays an important role. Any asymmetry causes warping and leads to measuring errors.

A cylindrical sample with a high length-to-diameter ratio is best suited for this study. Cast ZhS-6K rods were annealed at 1200 C for  $1.44 \times 10^{14}$  sec, and then samples produced on centerless polishing machines. The relationship of

change in length to number of cycles was investigated at 1000 C with air and water cooling. Length measurements were taken with vernier calipers. Data from the experiment are given in the table.

Начальная длина, мм (a)	Число циклов (b)	Конечная длина, мм (c)
-------------------------------	------------------------	------------------------------

Закалка на воздухе (d)

100,50	10	100,55
100,40	20	100,40
100,55	30	100,65
100,55	50	100,55
100,55	75	100,55
100,15	100	100,25
100,90	150	100,90
100,20	250	100,25
97,50	400	97,60
97,85	400	97,80

Length of samples before and after thermal cycling: a--initial length, mm; b--number of cycles; c--final length, mm; d--air cooled; e--water quenched

Закалка в воду (e)

99,45	10	99,50
99,35	20	99,40
99,40	30	99,50
99,65	50	99,75
99,55	75	99,60
99,55	100	99,60
99,55	150	99,62
99,30	250	99,40

As a result of the investigation no changes of linear dimensions were observed. Changes of length (according to measurements) did not exceed 0.1 mm which is within the limits of experimental error.

The produced data gives positive proof that alloys with a high recrystallization temperature are not affected by thermal cycling with respect to change of linear dimensions. It is interesting to note that after 250 cycles and water quenching, samples broke without a noted change of length. Hot hardness of samples was measured on a standard VIM-1M unit after thermal cycling.

Samples for measurement of hot hardness were cut into 5-mm sections from rods with a diameter of 15 mm after casting and heat treated in the same manner as the 100-mm rods. The prepared samples were given 400 cycles from 200-1000-200 C with fan cooling. Holding time in the furnace was 240 seconds, and in air--60 seconds. Hot hardness readings were taken at 20, 200, 400, 600, 800, 900 and 20 C. Three measurements were taken on each sample at each temperature.

Hot hardness data are given in Fig. 1. The curve represent change of hardness with respect to number of cycles. As can be seen, the curve has an erratic nature. However, the first minimum and maximum points on the curve coincided for all temperatures. This testifies to the fact that change of hardness during thermal cycling is not manifested by thermal stresses but by changes in the fine crystal structure of the alloy.

Fig. 2 shows the relationship of the magnitudes of the minimums, maximums and initial hardness taken from curves similar to that in Fig. 1.

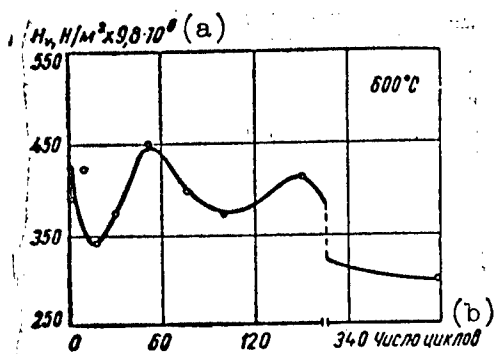


Fig. 1. Change of hardness with respect to number of cycles in alloy ZnS-6K: a--Vickers hardness,  $N/mm^2$ ; b--number of cycles.

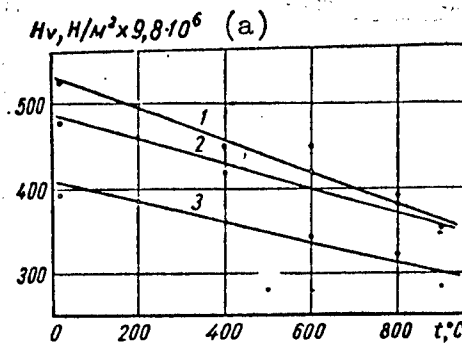


Fig. 2 Relationships of magnitudes of minimums, maximums and initial hardness: 1--initial hardness, 2--hardness of first maximum, 3--hardness of first minimum; a--Vickers hardness,  $N/mm^2$ .

Fig. 3 shows the change of eddy current loss as a function of number of thermal cycles in a ZnS-6K sample cycled at 1000 C and air cooled. From this study it was established that there is an increase in eddy current loss which may be associated with diminished electrical resistivity of the surface layer. However, the cause of the latter phenomenon is still unclear.

#### Relationship of electrical resistivity to number of thermal cycles in alloy ZnS-6K.

Electrical resistivity is a structure sensitive property, i. e., change of both structure and phase state is very finely defined by the change in its resistivity. This property is widely used for research of various types of heat treatment and among these is thermal cycling.

However, the method of electrical resistivity has one drawback in that it cannot be used to distinguish between changes of structure and phase composition especially when these changes are superimposed on each other. In such cases it is necessary to supplement the method of resistivity with the use of paramagnetic susceptibility which responds only to a change in phase composition.

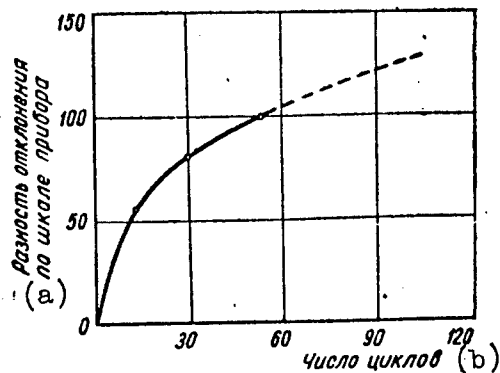


Fig. 3. Curve of change in eddy current loss as a function of number of cycles: a--difference in deflection of instrument; b--number of cycles.

Measurements of resistivity for alloy ZhS-6K were made using samples 3 mm in diameter and 100 mm long, which were subjected to thermal cycling (20-1000-20 C). A potentiometer with a standard PPTN bridge was used. Current and potentiometer leads were spot welded to the samples whereupon the distance between potentiometer leads was measured with a vernier caliper and sample diameter  $d$ --with a micrometer at several points. Resistivity  $\rho$  was calculated from sample resistance using the formula

$$\rho = R(\pi d^2/4l) \quad (1)$$

Measurements were taken at a constant temperature of 30 C which was maintained with the use of a thermostat. Accuracy of resistivity measurements was  $\pm 0.5\%$ .

A typical curve for change of resistivity with respect to number of thermal cycles is shown in Fig. 4, from which it is evident that in the initial stages  $\rho$  is decreased (up to 50 cycles). A second minimum is observed in the region of 300-350 cycles after which resistivity is continuously increased up to 600 cycles. As mentioned above, the curve of resistivity as a function of number of cycles is the result of the applied effect of two factors: 1) change of structure associated with change of stresses and block sizes and 2) change

of phase quantity and composition in the alloy. Nence, in order to understand processes which cause the produced relationship of resistivity to number of cycles it was necessary to compile the results of investigations by other methods along with this investigation. The study of paramagnetic susceptibility showed that in thermal cycling there is a continuous increase of susceptibility which denotes the continuous depletion of the matrix solid solution. The subsequent rise and plateau region of the curve can be understood by comparing the resistivity function with the hot hardness curve. In the same interval of cycles, a hot hardness peak is observed which apparently corresponds to reduced block dimensions. Consequently, in this interval the path of the resistivity curve is concurrent upon two factors: further depletion of the solid solution causing a lowering of resistivity, and breaking up of the mosaic blocks which then leads to an increase in resistivity.

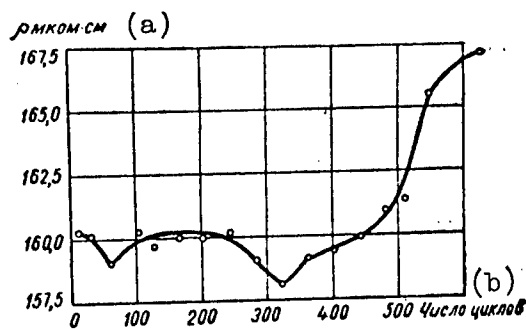


Fig. 4. Function of resistivity to number of cycles: a-- $\rho$ , microhms-cm; b--number of cycles.

The sharp rise of resistivity after 300 cycles is difficult to explain and can only be approached by comparison of hot hardness and paramagnetic susceptibility. For a precise explanation of these processes it will be necessary to find new methods using both structure sensitive properties and those properties which depend only on phase composition.

Paramagnetic susceptibility of samples and vanes of alloy ZnS-6K during thermal cycling.

The study of the phenomenon of thermal fatigue requires careful examination of structure and phase changes which take place in thermal cycling of alloys. In a number of works it

was shown that diffusion processes, which are accelerated by the combine effect of high temperature and cyclic stresses, lead to a more intense redistribution of elements between the grain and grain boundaries [17] and separation of phases in aging alloys [27], after which change of strength sets in. During extended holding at 900-1000 C, the  $\gamma'$ -phases and carbides are precipitated from alloy ZhS-6K.

A very effective method for studying phase transformations in alloys containing transition elements is measuring paramagnetic susceptibility. It is known that the paramagnetic susceptibility of a heterogeneous alloy X obeys the summation law:

$$X = \sum c_i \chi_i \quad (2)$$

where  $c_i$ --relative weight (or volume) of the constituent phases and  $\chi_i$ --their paramagnetic susceptibility. Summation is for all phases of the alloy. However, paramagnetic susceptibility of a phase depends on its composition. The change of transition element content in a phase causes a change of paramagnetic susceptibility. Thus, measuring paramagnetic susceptibility gives information on phase changes and on element redistribution in an alloy.

A device using a compensating method of measuring was developed and produced for measuring the paramagnetic susceptibility of alloy ZhS-6K. A diagram of the device is shown in Fig. 5. Sample 3 in special holder 2 is placed in a variable electromagnetic field 1. The non-uniform electromagnetic field is achieved by using ellipsoidal-shape tips. The sample is contained in a quartz suspension device.

As shown in work [37], the ellipsoidal-shape tips provide a constant stress field  $H$  at a magnitude of its gradient  $\partial H/\partial x$  in a plane perpendicular to the magnet axis and at a sufficiently large change of  $x$ . The resultant force is

$$F = \chi_m H (\partial H/\partial x) \quad (3)$$

where  $m$ --sample mass.

This force acts on the sample so long as the magnitude of  $\partial H/\partial x$  is not equal to zero which exists on the magnet axis. Therefore, if a sample has been placed at some distance from the magnet axis, then when the field is turned on it will move in a direction along the axis

In the described device, the suspension system was fastened with the aid of axle 6 in agate bearings 5 and had free movement around this axle, so that when the whole device was set up, its plane of oscillation was perpendicular to the axis of the magnet. When the sample was put into the device, it was at a distance of 10 mm from the magnet axis. When the magnet is activated the sample is moved in a direction toward its

axis up to the point where the sample will be in equilibrium between force  $F$  and the force of gravity (the arc described by this movement will be angle  $\alpha$ ). The compensation method consists in that upon the action of force  $F_1$  of opposite sign, the sample is returned to its initial position. At this time it is assumed that the value of the given force  $F_1$  or a proportional magnitude is known. The sample is returned to its initial position when  $F_1 = F$ . Then on the basis of equation (3), knowing the value of  $H$ ,  $\partial H/\partial t$ , it is possible to determine the paramagnetic susceptibility of the sample. However, determining  $H(\partial H/\partial x)$  is much more difficult. It is much more reliable and simple to measure susceptibility of samples of alloys which are of the same material for which the susceptibility is known.

To create a compensating force  $F_1$  in the device a system was examined which consisted of two permanent magnets 8 and coil 9, wound on a duraluminum frame, which acted as a damper. Coil power supply came from filament batteries and were regulated by a potentiometer. With the poles located as shown in Fig. 5, transmission of direct current to the coil, the coil attempts to move out of the field in the direction opposite to that of the current flow. The direction of the current is selected in such a manner so that the force acting on the coil moved the sample in a direction opposite to that in the magnetic field. Position of the sample is fixed by a system consisting of an illuminator 10, mirror 7, and microscope 11 in which the initial position of the sample is marked.

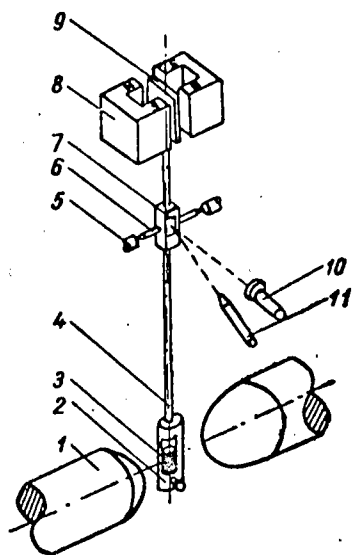


Fig. 5. Diagram of unit for measuring paramagnetic susceptibility.

Thus, paramagnetic susceptibility is measured on the described unit in the following manner. With the microscope the initial position of the suspension device with the sample is marked. A rectifier, supply power to the coil of the electromagnet, is turned on. Passage of current through the coil of the compensating instrument tries to return the sample to its initial position. The measure of force returning the sample is current  $I$  passing through the coil. This current is corrected to the unit mass of the sample and in this way serves to measure its paramagnetic susceptibility. Palladium was selected as a standard to determine sample susceptibility. It possesses high susceptibility

( $\chi = 5.3 \times 10^{-6}$ ), according to literature data [47]. Then, if  $i_o$ --calculated per 1 kg, is the compensating current for the sample, and  $i_{Pd}$ --the same for palladium, the paramagnetic susceptibility of the sample  $\chi_m^o$  can be easily found from the relationship:

$$\frac{i_o}{i_{Pd}} = \frac{\chi_m^o}{\chi_m^{Pd}} \quad (4)$$

Measurements showed that the error in determining  $\chi$  does not exceed 1.5%. Samples for measuring paramagnetic susceptibility were cylinders 3 mm in diameter and 7-11 mm long. The paramagnetic susceptibility of alloy ZhS-6K was investigated on samples of two types: 1) cast rods with a diameter of 3 mm which were given a standard heat treatment and then subjected to thermal cycling, and 2) samples cut from vanes which had past stand tests. At the same time vanes from different heats were tested. The results obtained on vanes from the material of one heat were in better agreement in that there was no variation of composition. In Fig. 6a and 6b, the topography is shown as to how the samples were cut from the vanes. As we see, the leading edge of the vane and the region adjacent to it, on both the "back" and "trough" sides, were investigated. Furthermore, susceptibility was measured in three places along the length of the vane. Selection of the indicated topography was dependent on the fact that cracks in vanes most frequently appear on the leading edge and are propagated into the vane. The study of paramagnetic susceptibility in relation to the number of thermal cycles, conducted in the mode of 20-1000-20 C and with air-jet cooling, revealed a continuous growth in susceptibility magnitude. This steady increase of susceptibility indicates that during thermal cycling there is a continuous redistribution of components between phases diminishes as number of cycles increases. No peculiar anomalies are observed in change of susceptibility which apparently denotes a smooth redistribution of elements and separation of new phases in the given conditions. True, the method of paramagnetic susceptibility does not make it possible to judge local changes of concentration which can occur in a sample. Therefore, the conclusion, which one can make from the results of measurements, belongs to the entire volume of the sample in this case. This conclusion consists of the following. Thermal cycling with air-jet cooling, carried out on thin ( $d=3$  mm) samples, apparently leads to an acceleration of aging processes, which should take place at the maximum temperatures of the cycle.

In vanes which have a more complex shape, a significant stress gradient, leading to ununiform redistribution of ele-

ments, is formed. Under these conditions, formation of cracks is more probable. Consequently, to study crack formation it is necessary to measure susceptibility very close to the cracks. Therefore, if cracks were observed in the vane, samples, besides those illustrated in Fig. 6, were also cut from sections adjacent to the crack.

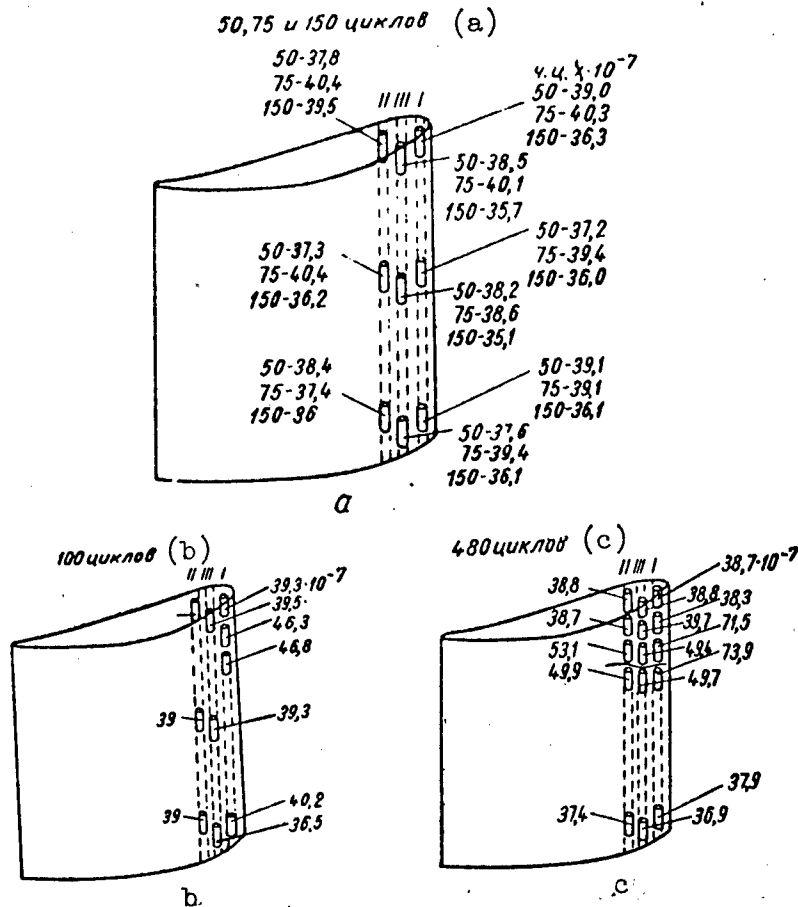


Fig. 6. Paramagnetic susceptibility at various points of a vane for different number of cycles: a--50, 75, and 150 cycles; b--100 cycles; c--480 cycles.

Vanes made from the material of one heat were studied after stand testing for 50, 75, 100, 150, 240, 350 and 480 cycles. In this case, cracks of different magnitude were observed in vanes after 100, 240, 350, and 480 thermal cycles. Measurements showed that the same regularity of change in sus-

ceptibility, with respect to number of cycles, is not observed in samples cut from the same sections of the vane (Fig. 6a--6c). It may even indicate the tendency of the studied sections to an increase of susceptibility up to 100 cycles, to a subsequent decrease susceptibility and a new increase starting at 350 cycles. However, it must be noted that susceptibility is the same for various sections of the vane along its length. As a rule, the highest susceptibility is observed in the top portions of the vane, especially during those cycles where the general increase in susceptibility is observed. It can be assumed that because of the non-uniform distribution of temperature along the vane during stand tests, there is a redistribution of alloying elements between phases which leads to increased susceptibility in the top portions of the vane. We noted that in all the examined vanes having cracks, these cracks were primarily located in the top portion. Thus, samples, cut from the section adjacent to a crack, have a notably higher susceptibility than the rest of the vane. For vanes after 480 cycles (Fig. 6c), a sample, cut from the edge close to a crack, shows a susceptibility of  $73.9 \times 10^{-7}$  while in sections further away from the crack this value is  $37\text{--}39 \times 10^{-7}$ . Here the increase of susceptibility depends on to what extent is a crack developed. In a vane after 100 cycles where crack development is just starting, susceptibility of the adjacent section is only  $46\text{--}47 \times 10^{-7}$  (Fig. 6b). Since cracks primarily form in the leading edge and, according to increase of number of cycles, are propagated inwardly, it is interesting to trace the change of susceptibility. It is evident in Fig. 6c that, for samples cut near cracks and in the deeper sections, susceptibility dropped to  $50 \times 10^{-7}$ , i. e., by 30%. Inasmuch as an increase of susceptibility is observed only in samples directly adjacent to the crack, while in neighboring regions no increase of susceptibility is observed, it is desirable to explain to what depth of a crack is the zone of increased susceptibility propagated. For this purpose a sample touching the crack was cut off little by little from the side of the crack and the susceptibility of the remaining section measured. Since susceptibility is calculated by the summation law, then

$$m_i \chi_i = m_l \chi_l + m_r \chi_r \quad (5)$$

where  $m_i$ ,  $m_l$ , and  $m_r$ —masses of the initial sample, the removed layer, and the remainder respectively, and  $\chi_i$ ,  $\chi_l$  and  $\chi_r$ —their susceptibility.

Using this formula, it is possible to calculate the susceptibility of the removed layer and, taking the susceptibility of this layer equal to the susceptibility of its center (which is true for thin layers), to plot a curve of the susceptibility

distribution along the depth of the sample, starting from the crack. This experiment was carried out for samples from a vane which had undergone 480 thermal cycles. Results of the experiment are shown in Fig. 7. As can be seen from the curve, the susceptibility of a crack is approximately 35 times greater than the average susceptibility of the vane material and diminishes rapidly to a depth of 0.5 mm. This drop of susceptibility slows down and at a depth of 1.2 mm the susceptibility is only 1.5 times greater than the initial material. Thus it has been explained that increased susceptibility is localized at a crack in the layer which does not exceed more than 2-2.5 mm. The cause of increasing susceptibility at a crack can be both redistribution of elements between phases near the crack and burn-out of elements from the crack surface which in this sense is the same for the surface of the vane.

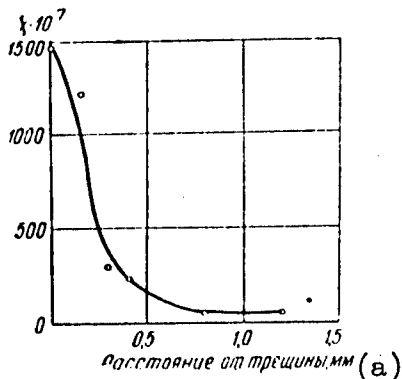


Fig. 7. Curve of the distribution of paramagnetic susceptibility to depth of sample: a--distance from crack, mm.

Thus, the study of paramagnetic susceptibility of alloy ZhS-6K during thermal cycling showed that for 3-mm samples the susceptibility increases uniformly and is the result of aging processes. No anomalies in this case (within the limits of experimental accuracy) are observed which, apparently, was a result of an almost complete absence of a thermal stress gradient during cooling. In samples cut from vanes, the susceptibility is unequally distributed in the body of the vane, whereupon, as a rule, it increases in the top third. An increase of susceptibility can be the result of depletion of the solid solution

with alloying elements which are transformed into the  $\gamma'$ -phase and carbides. We noted that cracks, as a rule, are formed in the top portion of a vane on the leading edge and form a zone having increased paramagnetic susceptibility.

Measurements of paramagnetic susceptibility during thermal cycling of alloys and vanes from alloy ZhS-6K reveal the important role of phase transformations which take place during such treatment. A further study of paramagnetic susceptibility will make it possible to explain the manner in which redistribution of elements between phases occurs during thermal cycling.

## BIBLIOGRAPHY

1. D. Lardzh, Zharoprochnyye Metallicheskiye Materialy (Heat-Resisting Metal Materials), Moscow, Foreign Literature Publishing House, 1958.
2. I. Ya. Dekhtyar, E. G. Madatova, Sbornik Voprosy Fiziki Metallov i Metallovedeniya (Problems of Metal Physics and Metal Science--Collection of Works), No 9, p 162, 1958.
3. H. Beisswenger, and E. Wachtel, Z. Metallkunde, Vol 46, No 50, 1955.

6368  
CSO: 1879-D/PE

N. P.

STUDY OF THE DIFFUSION AND OXIDATION  
PROCESSES IN ALLOY ZHS-6K UNDER  
CONDITIONS OF THERMAL CYCLING

[Following is a translation of an article by S. D. Gertsriken (deceased), I. Ya. Dekhtyar, L. M. Kumok, V. V. Pilipenko, and M. S. Khasanov in the Russian-language Voprosy Fiziki Metallov i Metallovedeniya (Problems of Metal Physics and Metal Science), Collection of Scientific Works of the Institute of Metal Physics, No 17, Kiev, 1963, Academy of Sciences Ukrainian SSR, pp 132-137.]

[The outstanding achievements of modern science and engineering still have the problem of the use of structural materials at elevated and super-high temperatures. The solution of thermal fatigue problems is especially important in connection with the construction of jet engines and flying apparatus of different action and in connection with the use of atomic and thermonuclear energy where the operation of components is associated with temperature fluctuations.]

[The number of cycles of heating and cooling until the appearance of cracks serves as a measure of thermal fatigue.] V. I. Arkharov [17], in studying the dynamics of crack development by x-ray analysis, noted that crack development precedes the formation of a block structure and turning and bending of blocks (investigations were conducted on a single crystal of aluminum). It is necessary to assume that diffusion processes play a significant, if not specific, role dependent on the combined effect of high temperature and cyclic stresses. They lead to precipitation of a second phase (carbides and intermetallides) in a finely dispersed state and to redistribution of elements between the body of a grain and the boundary zones and have a decisive effect on strength of a material.

[As a rule, thermal cycling shows a negative effect on]

(the mechanical properties of a material. Long-time strength is diminished with increase in number of cycles. Processes of material fracture or change of part shape are very complex and their development depends on a whole series of reasons which are dependent on the nature of materials and alloys, on the parameters of a thermal cycle and other factors.

Corrosion of a material has much significance as to thermal stability. As is known, corrosion involves formation of stress concentrators which lead to deterioration of thermal stability.

Diffusion of Chromium and nickel in alloy ZhS-6K by methods of vaporization in a vacuum and radioactive isotopes.

If one of the components in an alloy has a relatively high vapor tension, then during heating in a vacuum it will be easily vaporized. In this case a concentration gradient will develop this component will be vaporized from the surface to the point that there will be a movement of the material to the surface by means of diffusion. Taking into account the quantity of material vaporized, one can determine the diffusion coefficient of a component with a high value of vapor tension.

Calculations of the coefficients of diffusion were done by formulas derived by Grinberg and then refined and tabulated by Gertsriken and his associates [47]. Knowing the percentage content of chromium in the alloy, it is possible to determine its absolute content  $Q_0$  in a given sample. The change of weight of a sample  $\Delta m$  in the process of annealing at temperature  $^{\circ}K$  in time  $t$  we assume to occur due to vaporization the chromium. Hence, as a result of annealing,  $Q_0 - \Delta m = Q$  chromium remains in the sample. Knowing  $Q/2Q_0$ , it is possible, in accordance with the given method, to find  $D_t/h^2$  from tables, where  $h$  is the half-thickness of the sample. This is how the diffusion coefficients of chromium were found for five temperatures in the interval 1273-1423 K.

T, $^{\circ}K$	1273	1323	1373	1398	1423
D, $m^2/sec$	$3.16 \times 10^{-16}$	$2.52 \times 10^{-15}$	$9.33 \times 10^{-15}$	$1.91 \times 10^{-14}$	$3.98 \times 10^{-14}$

To determine the activation energy of the diffusion process the temperature relationship of the diffusion coefficient was used, which has the form

$$D = D_0 e^{-(E/RT)} \quad (1)$$

where  $E$ --activation energy,  $T$ --absolute temperature,  $R$ --gas constant, and  $D_0$ --factor independent of temperature. Taking

the logarithm of this equation we obtain

$$\ln D = \ln D_0 (-E/R)(1/T), \quad (2)$$

and from this it is evident that  $\ln D$  is a linear function of reciprocal temperature on the Kelvin scale. In this manner, by plotting the relationship of  $\ln D$  to reciprocal temperature (Fig. 1), we determine the activation energy of diffusion and the entropy member  $D_0$ . As a result the following relationship of the diffusion coefficient of chromium in alloy ZhS-6K to temperature was obtained:

$$D = (1.01 \times 10^4) e^{-(477 \times 10^3/RT)} \text{ m}^2/\text{sec} \quad (3)$$

The high value of diffusion activation energy in the investigated alloy and its relatively low diffusion coefficient indicate that this alloy should be stable to weakening at elevated temperatures.

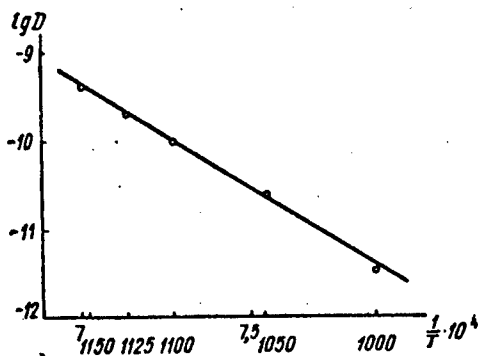


Fig. 1. Relationship of the diffusion coefficient of chromium to reciprocal temperature in alloy ZhS-6K.

In the case of studying the diffusion of radioactive  $\text{Ni}^{63}$ , which has a very soft  $\beta$ -radiation ( $1.01 \times 10^{-14}$  joules), it is convenient to use the absorption method. This method is based on the use of change of sample activity before and after annealing due to radiation absorption of the diffusing element owing to its penetration into the sample. Diffusion annealing of samples was carried out in a quartz tube which was evacuated and then filled with argon after which it the tube was placed in an electric furnace.

The diffusion coefficient was calculated by the formula

$$N_t/N_0 = e^{-z^2} \text{erf } z \quad (4)$$

where  $z^2 = \mu^2 Dt$ ;  $N_0$ --integral activity of the sample before annealing; and  $N_t$ --integral activity of the sample after annealing for period of time  $t$ .

Gertsriken and Pryanishnikov compiled tables with the aid of which, knowing  $N_t/N_0$ , it was possible to find  $z = \mu \sqrt{Dt}$ , and then knowing  $\mu$  and  $t$ , to find  $D$  where  $\mu$  is the coefficient of absorption for  $Ni^{63}$  radiation in the investigated sample.

To determine the absorption coefficient and radiation of nickel in the alloy, the following formula was used:

$$\mu = \frac{\mu_1 c_1 + \mu_2 c_2 + \mu_3 c_3 + \dots}{100} \quad (5)$$

where  $\mu_1, \mu_2, \mu_3 \dots$ --coefficients absorption for nickel radiation in the corresponding components of the alloy, and  $c_1, c_2, c_3$ --percentage of these components in the alloy. The absorption coefficients can be determined if one of them is known by the ratio  $e_1/e_2 = \mu_1/\mu_2$ , where  $e_1$  and  $e_2$ --density of the respective components. For the initial magnitude of the absorption coefficient of nickel radiation in nickel, we used  $10^5 m^{-1}$ . On the basis of calculations by the indicated method, an absorption coefficient of  $9.88 \times 10^4 m^{-1}$  was obtained.

Diffusion coefficients were calculated as the average value of 2-3 annealing times for 2-4 samples.

T, °K	1093	1173	1293	1393
D, m <sup>2</sup> /sec	$4.65 \times 10^{-15}$	$11.71 \times 10^{-15}$	$3.44 \times 10^{-14}$	$8.95 \times 10^{-14}$

Activation energy of the process E and  $D_0$  were determined from the graph of the relationship between  $\ln D$  and  $1/T$  which ensues from equation (1).

Thus, the diffusion equation takes on the form

$$D = (0.324 \times 10^{-8}) \exp (161 \times 10^3 / RT), \text{ m/sec.} \quad (6)$$

The large diffusion coefficients and low activation energy show that in the given case the granular diffusion plays an important role. This is very important for a subsequent explanation of processes which take place in the given alloys under conditions of high temperature operation.

#### Isothermal oxidation of alloy ZhS-6K.

To study isothermal oxidation of the alloy a special unit was developed which made it possible to weigh the sample

without removing it from the furnace. In this manner it was possible to anneal the sample with constant observation of its change in weight as a result of oxidation.

On the basis of measurements, time functions of the change in sample weight per square centimeter were obtained for three temperatures: 1273, 1373, and 1473 K. A typical relationship for  $T = 1473$  K is given in Fig. 2.

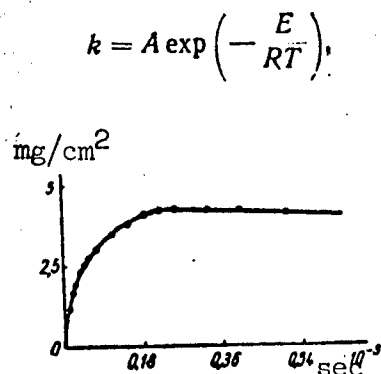


Fig. 2. Time function of sample change in weight per square centimeter in the case of isothermal heating at 1473 K

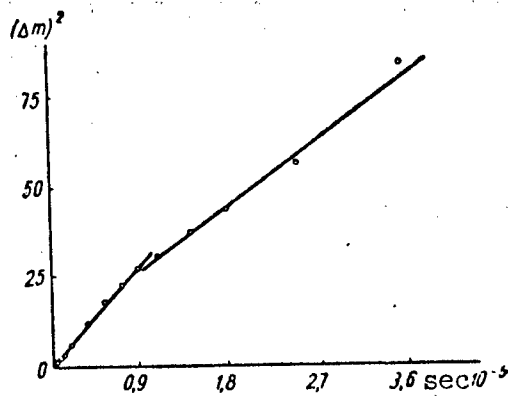


Fig. 3. Time relationship of the square of change of weight of samples per square centimeter in the case of isothermal heating at 1373 K

It was shown that the points of these curves satisfy the parabolic law of oxidation  $(\Delta p)^2 = kt + c$ , where  $p$  -- change in sample weight in the process of oxidation relative to one square centimeter;  $k$  -- oxidation constant; and  $c$  -- constant for the parabolic equation.

During the time of oxidation, the magnitude of  $k$  is changed somewhat (Fig. 3). Corresponding magnitudes are given in Table 1.

After oxidation for five hours at 1473 K, no further change in sample weight is observed. This is evidently the result of the formation of a thick oxide layer which prevents further oxidation.

An evaluation of the activation energy of the process was conducted for two temperatures (1273 and 1373 K), because the time continuity of the oxidation constant at 1473 K is not comparable for the other two temperatures. For this, the relationship

$$k = A e^{-(E/RT)} \quad (7)$$

was used where  $A$  is the temperature independent parameter and

$E$  is the activation energy of the process. The activation energy of the process was found to be 71.2 kilojoules/mole.

Table 1

$T, K$	Промежуток времени, в сек, где (a) $k = \text{const}$	$k, \frac{\text{mg}^2}{\text{sec}}$
1273	0,36	$1,53 \cdot 10^{-4}$
	0,36—1,8	$1 \cdot 10^{-4}$
1373	0—0,9	$3,3 \cdot 10^{-4}$
	0,9—4,5	$1,97 \cdot 10^{-4}$
1473	0—0,054	$14,7 \cdot 10^{-4}$
	0,054—0,18	$7,73 \cdot 10^{-4}$
	0,18—3,6	$0,00 \cdot 10^{-4}$

Key: a--intermediate time in seconds where  $k = \text{constant}$ ;

#### Oxidation of alloy ZnS-6K during cyclic annealing.

In contrast to the case of isothermal heating, in cyclic heating there occurs a loss of weight of the samples. At this time oxidation strongly depends on selection of the mode of cyclic heat treatment.

Thus, at 1373 K with various cycling times of  $86.4 \times 10^3$ ,  $21.6 \times 10^3$ ,  $3.6 \times 10^3$ , and  $0.9 \times 10^3$  seconds the rates of oxidation will be  $0.834 \times 10^{-5}$ ,  $2.21 \times 10^{-5}$ ,  $20.8 \times 10^{-5}$ , and  $83.4 \times 10^{-5}$   $\text{mg}/\text{cm}^2\text{-sec}$  respectively. This relationship is shown in Fig. 4.

Weight of samples during cyclic annealing decreases due to break-off of oxides at the moment of a sharp change of temperature, which, in turn, proceeds as a result of the difference in expansion coefficients of the scale and the initial material. At temperatures of 1273 and 1473K, oxidation was conducted at  $0.9 \times 10^3$  seconds per cycle with  $0.2 \times 10^3$  sec for air cooling. The oxidation rate for a specific time was different for different temperatures and remained almost constant for the indicated temperatures which respectively were equal to  $0.0528 \times 10^{-4}$  and  $19.9 \times 10^{-4}$   $\text{mg}/\text{cm}^2\text{-sec}$ .

Comparison of these data with data on the oxidation of nichrome in conditions of cyclic heat treating at 1373 K showed that the oxidation rate of alloy ZnS-6K is approximately 1.5 times less than that for nichrome at the same conditions.

X-ray analysis was used to study the phases of the oxides

of vanes having been in operation for  $7.2 \times 10^5$  seconds. It was found that into the composition of the oxides, both nickel and chromium enter. For this x-ray diffraction patterns were taken of powders from the investigated alloys. On the patterns were noted lines characteristic for different phases.

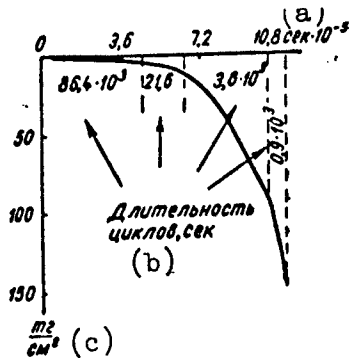


Fig. 4. Time relationship of sample change in weight per square centimeter in the case varying the process of cyclic oxidation at 1373 K: a--seconds; b--cycle time, seconds; c--mg/cm<sup>2</sup>.

In Table 2 are given the values of  $l$  and  $\sin \varphi$  for the identified lines corresponding to the NiO phase.

Table 2

$l$	$a \cdot 10, \text{nm}$ (a)	$hkl$	$\sin \varphi$ (теор.) (b)	$2l, \text{mm}$	$\varphi \cdot 10^2, \text{rad}$ (c)	$\sin \varphi$ (экспер.) (d)
12	4,172	(222)	0,947	36	125,0873	0,953
24	4,172	(311)	0,906	48	115,61	0,916
100	4,172	(200)	0,547	67,5	58,535	0,554
60	4,172	(111)	0,476	56	48,513	0,467
60	4,172	(200)	0,775	79	88,08	0,772

Key: a--nm, b--(theoretical), c--radians, d--(experimental).

That the circumstance that the measured  $\sin \varphi$  did not precisely agree with calculated magnitudes of  $\sin \varphi$  in the assumption of a pure oxide NiO, it is apparent that in the formation of NiO, certain other elements enter into the alloy.

As can be seen from Fig. 4, lines for NiO are present. Another system of lines being present are those of chromium oxide.

#### BIBLIOGRAPHY

1. V. I. Arkharov, A. I. Semenov, Doklady Akademii Nauk SSSR (Reports of the Academy of Sciences USSR), Vol 83, No 8, 1952.
2. V. I. Arkharov, Doklady Akademii Nauk SSSR, Vol 88, No 3,

- 1953.
3. Ye. B. Brovchenko, A. A. Bochvar, Izvestiya Akademii Nauk, Otdeleniye Tekhnicheskikh Nauk (News of the Academy of Sciences USSR, Division of Technical Sciences), No 11, pp 10-13, 1957.
  4. S. D. Gertsriken, G. Il'kevich, I. Sakharov, and I. Fayngol'd, Zhurnal Tekhnicheskoy Fiziki (Journal of Technical Physics), Vol 10, No 10, 1940.

6368  
CSO: 1879-D/PE

- END -